CHEMICAL ENGINEERING TRANSACTIONS
VOL. 50, 2016
A publication of AIDIC
The Italian Association of Chemical Engineering
Online at www.aidic.it/cet
Guest Editors: Katharina Kohse-Höinghaus, Eliseo Ranzi

ISBN 978-88-95608-41-9; **ISSN** 2283-9216
DOI: 10.3303/CET1650054

Biodiesel Production Via Hydrodynamic Cavitation: Numerical Study of New Geometrical Arrangements

Jair Alexander Ladino[a],Jason Herrera[a],Dionisio H. Malagón[b],Marina Prisciandaro[d], Vincenzo Piemonte [c], Mauro Capocelli[c]

[a] School of Mechanical Engineering. Universidad del Valle, Cali. Colombia
[b] Department of Industrial Engineering, Universidad ECCI, Bogotá. Colombia
[c] Faculty of Engineering, Università Campus Biomedico di Roma, Rome, Italy
[d] Department of Industrial Engineering Ilipartimento di Ingegneria Industriale, dell'Informazione e di Economia, Università dell'Aquila, L'Aquila, Italy

v.piemonte@unicampus.it

Hydrodynamic Cavitation is employed as process enhancer for the industrial production of biodiesel with important improvements in energy efficiency, yields and required time. These improvements can play an important role in the new generation of biodiesel facilities, even more under the recent global scenario of low petroleum prices where the biodiesel industry is struggling to be competitive and economically sustainable. In this framework the cost and time reduction can be achieved overcoming the present limitations of low mass transfer coefficients and enabling the utilization of high fatty acid oils. This work explores via an integrated mathematical model (computational fluid dynamics and single bubble dynamics) several geometrical possibilities for cavitational reactors with simple construction and easy scalability as cylinders and Venturi channel arrangements. The paper presents the fundamental equations and the global simulation criteria integrating the multi-scale approaches for the evaluation of cavitation activities and power consumption in transesterification reactors. The preliminary results are presented in this paper, together with an innovative overall comparison including the different features characterizing the cavitation performances. Finally, the methodology applied to 16 configurations of Venturi and cylinder arrangements suggest that the cylinder arrangement named 4510 (array cylinders with throat diameter of 4mm and cylinder diameter of 5mm) has better overall performance at less energy consumption, reaching up to 95% of active cavities and an average performance of 60% compared with other evaluated geometries.

1. Introduction

The Cavitation is defined as the phase change of a liquid medium due to reduction of local pressure below the vapour pressure (Franc and Michel, 2005; Gogate et al., 2006) causing the nucleation and growth of microbubbles that, passing through higher pressure zones (the recovery zone or particular flow instabilities), collapse violently with extreme increments in pressure and temperature (Abdullah et al., 2012; Gogate et al., 2006). Although known for its negative consequences, e.g. erosion in turbomachinery parts such as turbine blades and guide vanes (Rodriguez et al., 2015) the cavitation phenomena can be harnessed as a process intensification in several fields: waste water treatment (Musmarra et al., 2016; Capocelli et al., 2014a), microorganism inactivation (Capocelli et al., 2014b), emulsification processes (Pandit and GaikWad, 2007) as well as biodiesel production (Abdullah et al., 2012). An essay on the Ultrasonic Cavitation potentiality in enhancing chemical-physical processes is given by Christian Horst in the book of Keil (2007). The uses of Cavitation for biodiesel production has been recently summarized by Ozonek in 2012 or, more in detail, by Feng et al., 2015.
The main peculiarities of cavitation in Process Intensification are the generation of a two phases (macroscopically) and the high turbulent regime increasing reaction rates and local heat and mass transfer coefficients (Pandit et al., 2008). These features provide a highly reactive system for the biodiesel transterification (Wang et al., 2006) by reducing the reaction time, increasing the yields, expanding the

Please cite this article as: Ladino J.A., Herrera J., Malagon D., Prisciandaro M., Piemonte V., Capocelli M., 2016, Biodiesel production via hydrodynamic cavitation: numerical study of new geometrical arrangements, Chemical Engineering Transactions, 50, 319-324
DOI: 10.3303/CET1650054

operating conditions and providing thermic self-sustainable reactions. Higher rate means smaller reactor size, shorter residence time and higher throughput in a given time. Moreover, by properly design the HC reactor, high concentration of Free Fatty Acids (FFA) like waste cooking oil, yellow and animal greases can be implemented as raw material reducing the energy consumption (Gogate et al.,2008). Biodiesel is the renewable counterpart of petro-diesel, it is the most used biofuel and is commonly blended with it to create BX (blend of x% biodiesel and (100-x %); the large scale production requires processes which have an economic competitiveness and a low environmental impact (Piemonte et al., 2014,2015). In general, it is one cent per gallon more expensive than diesel for every percent added mainly depending on the market price for vegetable oil. The feedstock price decreases as the free fatty acid content (FFAs) increase but processing cost also increases to make them suitable for base-catalyzed biodiesel production (Mahamuni and Adewuyi, 2010) with shorter reaction times, cheaper reagents and less extreme physical conditions, additionally leading to less expensive and smaller chemical plants (Boffito et al., 2015).
Hydrodynamic cavitation (HC) is generated in a cheaper, scalable and more energy efficient method than other methods as ultrasound (Gogate et al., 2008) by designing proper apparatus for the fluid flow constriction. The R&D results related to high efficient reactors are owned by the companies (Kozyuk, 2004; Gordon et al., 2010), and not fully available to the scientific community. On the other hand, the academic world is focused on both the experimental and modeling development of the fundamental investigations (physical and chemical effects) on simple geometries such as orifice plate and Venturi (Capocelli et al., 2014c). Up to now, there are few work related to more complex geometries (Pandit et al., 2015). Moreover, the majority of numerical works are based on Single Bubble Dynamics (SBD) with the assumptions of one dimensional flow, Bernoulli pressure determination and simple turbulent models for fluctuations for evaluating the collapse conditions (Capocelli et al., 2013) and few models can be found on CFD optimization (Pandit et al., 2011a-b; Tarash et al., 2014).
With this premises, we believe that modelling approaches based on CFD simulations are extremely needed in this field for investigating the effect of several operating and geometrical variables and to optimize complex system before the realization of laboratory apparatus or industrial pilot plants. Therefore, this work presents a criteria of geometrical optimization by coupling CFD simulations and SBD modeling applied to complex convergent-divergent geometries with the aim to determine the cavitational activity for several configurations. Thus, in this work, we describe the overall methodology based upon the cited studies (Pandit et al., 2011a-b; Tarash et al., 2014), we present the overall multiscale criteria for the performance evaluations and show the first preliminary results of the “CFD-optimization campaign” on sixteen Venturi-Cylindric arrays geometries.

2. Theoretical background

2.1 Fluid Flow Model

The cavitation phenomena for a turbulent flow can be modelled by the Continuity equation (Eq.1), the Reynolds Averaged Navier-Stokes equations (RANS) in Eq.2 and the transport equation (Eq. 3).

$$\partial_t \rho + \nabla \cdot (\rho v) = 0 \tag{1}$$

$$\partial_t (\rho v) + \nabla \cdot (\rho v \otimes v) = -\nabla p + \nabla \cdot \left(2\mu [D] - \rho \overline{v' \otimes v'}\right) \tag{2}$$

$$\partial_t (\rho_l \alpha_l) + \nabla \cdot (\rho_l \alpha_l v) = \phi_c - \phi_e \tag{3}$$

$$\partial_t (\rho k) + \nabla \cdot (\rho k v) = \nabla \cdot \left((\mu_t / \sigma_k) \nabla k\right) + 2\mu_k [D] \cdot [D] - \rho \varepsilon \tag{4}$$

$$\partial_t (\rho \varepsilon) + \nabla \cdot (\rho \varepsilon v) = \nabla \cdot \left((\mu_t / \sigma_k) \nabla \varepsilon\right) + C_{1\varepsilon} 2(\varepsilon / k) \mu_k [D] \cdot [D] - C_{2\varepsilon} \rho \left(\varepsilon^2 / k\right) \tag{5}$$

Where ρ is the density of the vapor-gas-liquid mixture and v is the mean component of the homogeneous field velocity, [D] is the mean strain rate tensor and the Reynolds Stress Tensor is modeled with the assumption of isotropic turbulence and the Boussinesq hypothesis (Vertseeg and Malalasekera, 2007) and closed with the two equation k-ε turbulence model (Eq. 4-5) and standard wall functions (Launder and Spalding, 1974). Finally, the source terms Φc and Φe are condensation and vapor generation rates respectively computed via the mass transfer model (Section 2.2).

2.2 Mass Transfer Model

At the macroscale, the problem is considered isothermal, the vapor density is computed via saturated vapor data and the liquid phase is considered constant. For mass transfer computation, the cavitation model is based on truncated linear Rayleigh Plesset Equation (Eq. 6) and the mass flow rate between phases is described by Eq.7 (Bakir et al., 2004).

$$d_t R_B = (2/3)\left[(p_v - p)/\rho_l\right]^{1/2} \tag{6}$$

$$\phi_{c,e} = F_{c,e} \cdot N_B \rho_v 4\pi R_B^2 \left[(2/3)|p_v - p|/\rho_l\right]^{1/2} \mathrm{sgn}(p_v - p) \tag{7}$$

Where R_B is the initial bubble radius, p_v is the vapor pressure inside the bubble at the liquid bulk temperature, p is the pressure field around the bubble, ρ_f is the liquid density, the empirical constant F takes into account for the different time scale of vaporization and condensation rates respectively (F_e=*50 and* F_c=*0.01*) and N_b is the number of bubbles per unit of volume related to the vapor volume fraction according to the literature (Bakir et al., 2004).

2.3 Bubble dynamics model

The dynamics of a spherical bubble (microscale) is given by the Rayleigh-Plesset equation (Eq. 8), where σ_{st} is the surface tension coefficient. The pressure inside the bubble $p_B(t)$ is the sum of vapor pressure p_v and gas pressure of non-condensable gas $p_g(T)$ (Eq. 9) in which p_{g0} is the equilibrium state gas pressure (at reference-initial radius R_0). During the growth phase, the process is assumed isothermal with a unitary ratio of specific heats; during the collapse, which is very fast, the process is assumed as adiabatic (isentropic) with γ=1.41(Vallier, 2013).

$$R d_t^2 R + (3/2)(d_t R)^2 = \left(p_B(t) - 4\mu_l (1/R) d_t R - 2\sigma_{st}/R - p(x_B,t)\right)/\rho_l \tag{8}$$

$$p_g(t) = p_{g0}\left(R_0/R(t)\right)^{3\gamma} \tag{9}$$

Finally, the surrounding pressure $p(x_B,t)$ is obtained from the CFD macro model simulations taken by time history of mean bulk pressure p_{Bulk} for each streamline and the turbulent pressure assumed by a sine function with amplitude and frequency computed from turbulent kinetic energy k and dissipation rate ε (Eq. 10) (Pandit et al., 2011a).

$$p(x_B,t) = p_{Bulk}(x_B,t) - (\rho k/3)\sin(2\pi(\varepsilon/k)t) \tag{10}$$

2.4 Multiscale model

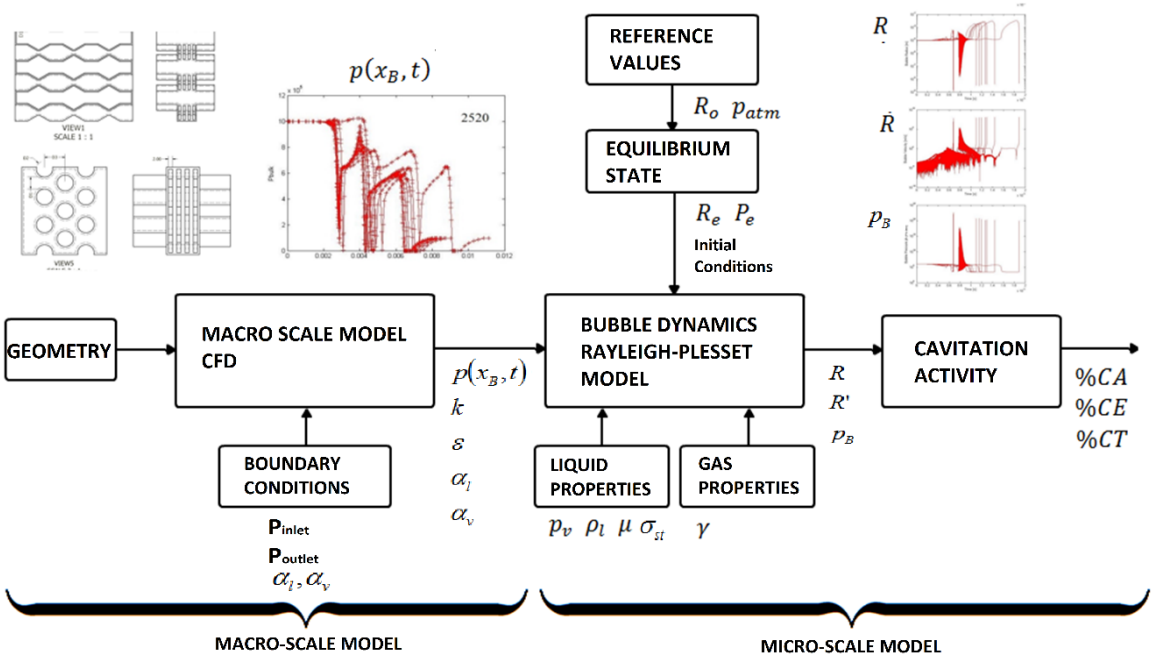

Figure 1 Multiscale Algorithm for evaluation of hidrodynamic cavitation

The multiscale algorithm is presented in Figure 1. The overall methodology proposed consists of two main steps: a macro scale modelling of CFD two phase Eulerian-Eulerian simulations and a micro scale modelling of Single Bubble Dynamics (SBD) to determine the transient behavior of each bubble crossing the cavitation chambers, based on the pressure profile of the first stage. Boundary conditions are the pressure differences in the inlet-outlet of cavitation chambers, initial volume fractions, vapor pressure and initial cavity radius. The

solution is performed via ANSYS-CFX® software. The output of simulations (at the macro scale) are mainly the pressure, liquid and vapor fraction fields and streamline patterns (assumed as the cavity pathways). The mean pressure temporal profiles, turbulent kinetic energy k and rate of dissipation ε recorded along each streamline, are used as the inputs of the microscale model (Eq. 10). In the SBD, the Eq. 9 is divided into a system of first order non-linear stiff ODE for the bubble radius $R(t)$ and interface velocity $R'(t)$ evolution. Numerical solution is achieved via MATLAB® ODE15s variable order, multistep solver based on numerical differentiation formulas. The final results are the bubble radius, interface velocity and pressure as function of time. The initial conditions considered for evolution of cavities are defined in order to avoid spurious oscillations at the initial steps of the simulations (Vallier, 2013). The final stage is the result processing for the evaluation of geometry performances, *e.g.* the determination of cavitational activity (if p_B>>10 p_{in}) according to the criteria given by Pandit et al., 2011a-b. The methodology of simulation was applied for the evaluation of cavitational behavior of geometries like Venturi and Cylinder arrangements Figure 2, with the main dimensions reported in **Errore. L'origine riferimento non è stata trovata.**.

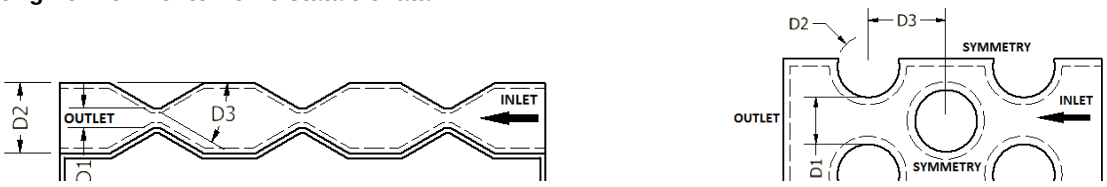

Figure 2 Schematic view of geometry arrays modeled for Venturi (Left) and Cilinder Array (Right)

Table 1: Nomenclature and dimensions of the investigated geometries

Venturi	**2630**	**2660**	**2830**	**2860**	**4630**	**4660**	**4830**	**4860**
D1 Throat width [mm]	2	2	2	2	4	4	4	4
D2 Venturi width [mm]	6	6	8	8	6	6	8	8
D3 Reduction angle [Deg]	30	60	30	60	30	60	30	60
Array cylinders	**2510**	**4510**	**2520**	**4520**	**21010**	**41010**	**21020**	**41020**
D1 Throat width [mm]	2	4	2	4	2	4	2	4
D2 Cylinder diameter [mm]	5	5	5	5	10	10	10	10
D3 Cylinder Pitch [mm]	10	10	20	20	10	10	20	20

3. Results and Discussion

All macro scale simulations were performed for different inlet pressures (4,7,10,13 bara) and outlet pressure set to 1bar. Figure 3 shows the typical velocity and pressure field for a CFD simulation over a cylinder array (4510). These results represent the input of the SBD simulation for the evolution of $R(t)$, $R(t)'$ and temperature/pressure of the bubble. The example of SBD output is given in Figure 4 showing the evolution of the bubble radius and pressure for the cylinder configuration 4510 (reaching the minimum cavitation number Cv = 0.09). Although the nominal values are not relevant since SBD does not account for bubble compressibility and bubble-bubble interaction, the model enables the determination of active cavities for configurations studies. The reactor performance is eventually determined by the following parameters.

- Percentage of active cavities (AC);
- Percentage of average vapour volume fraction (AVF);
- Complement of Cavitation Number (1 - C_v);
- Number of Unit (parallel cavitational arrays) needed per a unit of Flow Rate (unit per flow rate, UPF);

For comparison purposes, all parameters have been normalized for each configuration and averaged. Configuration with the highest average values are 4510, 41010 and 4630 (Table 1). In particular, the configuration 4510 has the highest average which, under the investigated pressure range, is able to operate at the lowest C_v, with the highest percentage of active cavities (95.2%), a substantial extension of the vapour zone and less parallel arrays required to process a unit of flow rate (in the order of 2 arrays) compared with other configurations. Therefore, by presented criteria, the 4510 configuration is the most energy efficient, obtaining better operational conditions than others with the same power per unit of flow rate of 900 W/(l/s).

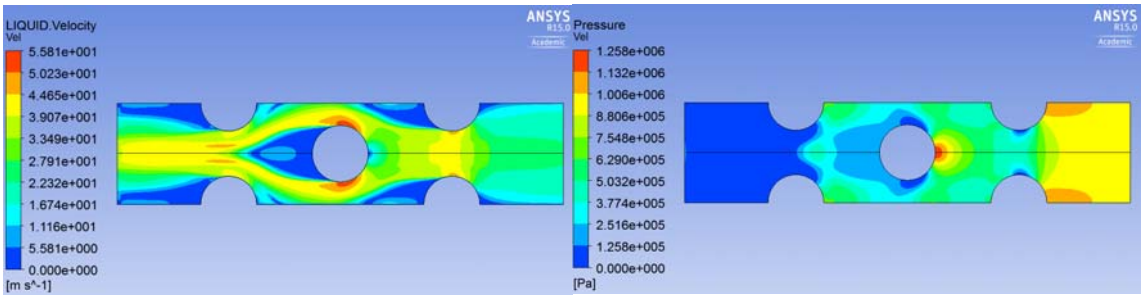

Figure 3 CFD simulation (macroscale) for the cylinder array named 4510, cavitation number Cv 0.09.

Table 1 Reported values of high score geometries

Reference	Cv	AC [%]	AVF [%]	$(1-C_v)$[%]	$(UPF)^{-1}$[%]	Average [%]
4510	0.062	95.2	8.1	93.8	44.6	60.4
41010	0.058	80.0	13.0	94.2	46.4	58.4
4630	0.101	95.4	5.11	89.9	35.0	56.4

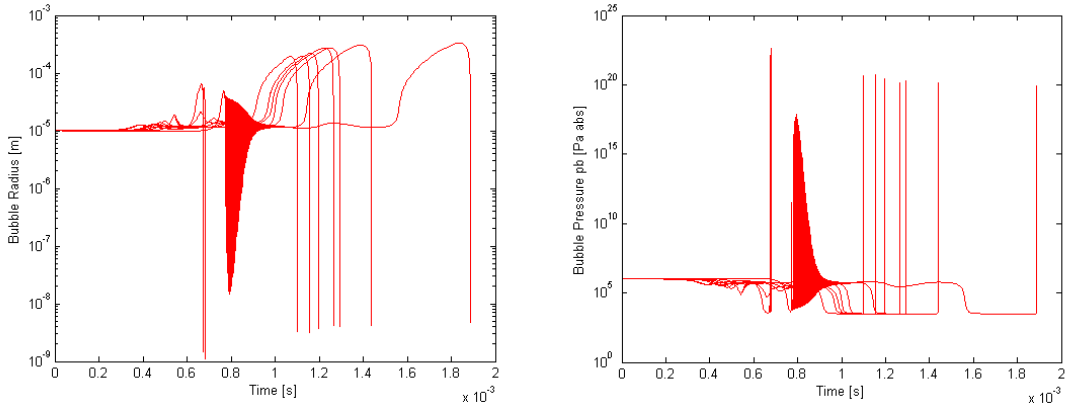

Figure 4 Evolution of bubble radius R(t) and pressure for reference 4510 Cv 0.09 for determination of active cavities.

4 Conclusions

Numerical simulations at multiscale level were performed using cavitation model and mass transfer model at the macroscale and single bubble dynamics at the microscale for bubble behaviour based on Rayleigh Plesset equation for bubbles moving along the flow streamlines (assumed as the bubbles paths). Mean pressure profiles, vapour volume fraction and bubble radius, pressure and wall velocity were monitored and used to evaluate the overall cavitational performance of the analysed cavitation chamber. A new evaluation methodology was proposed and based on percent of active cavities (measure of cavitational intensity), percentage of average vapour fraction (as measure of cavitational size), complement of cavitation number and Number of parallel cavitational arrays needed per unit of flow rate as indicators of the overall energy efficiency. This methodology was applied to the sixteen geometries proposed and the best results (obtained for the cylindrical arrangement configuration 4510) have been described. The proposed criterion seems to be a useful tool for the conceptual optimization of new geometries accounting for the cavitational intensity as well as other process variables measuring the chamber efficiency and size for a given flow rate.

Further work can be extended to obtain accurate simulations including compressibility effects, chemical reactions, heat transfer and phase mass transfer for the biodiesel applications. Further improvements may also include the evaluation of bubble interaction and Nuclei size distribution.

Reference

Abdullah, A., Salamatinia, B. & Bhatia, S., 2012. Quality evaluation of biodiesel produced through ultrasound-assisted heterogeneous catalytic system. Fuel Processing Technology journal, Volume 97, pp. 1-8.

Bakir, F. et al., 2004. Numerical and Experimental Investigations of the Cavitating Behavior of an Inducer. International Journal of Rotating Machinery, Volume 10, pp. 15-25.

Boffito , D. et al., 2015. Transesterification of Triglycerides in a New Ultrasonic Assisted Mixing Device. Chemical Engineering Transactions, Volume 43.

Capocelli, M., Prisciandaro, M., Musmarra, D. & Lancia, A., 2013. Understanding the Physics of Advanced Oxidation in a Venturi Reactor. Chemical Engineering Transactions, Volume 32.

Capocelli, M., Prisciandaro, M., Lancia, A. & Musmarra, D., 2014.a Hydrodynamic cavitation of p-nitrophenol: A theoretical and experimental insight. Chemical Engineering Journal.

Capocelli, M., Prisciandaro, M. & Lanci, A., 2014b. Comparison Between Hydrodynamic and Acoustic Cavitation in Microbial Cell Disruption. Chemical Engineering Transactions, Volume 38, pp. 13-18.

Capocelli, M., Musmarra, D., Prisciandaro, M. & Lancia, A., 2014c. Chemical effect of hydrodynamic cavitation: simulation and experimental comparison. AiChe J, 60(7), pp. 2566-2572.

Gordon, R., Gorodnitsky, I. & Promtov, M., 2010. Multi-stage cavitation device. Cavitation Technologies, Inc, USA, Patent No. US20100290307 A1.

Fang, Z., Smith, R.L.Jr., Qi, X., 2015. Production of Biofuels and Chemicals with Ultrasound. Springer Science, Dordrecht

Kozyuk, O., 2004. Device and method for creating hydrodynamic cavitation in fluids. Five Star Technologies, Inc. USA, Patent No. US7207712 B2.

Gogate, P., Tayal, R. & Pandit, A., 2006. Cavitation: A technology on the horizon. CURRENT SCIENCE, pp. 35-46.

Gogate, P. R., 2008. Cavitational reactors for process intensification of chemical processing applications: A critical review. Chemical Engineering and Processing, Volume 47, p. 515–527.

Franc J-P, Michel J. -M. , 2005. Fundamentals of Cavitation. s.l.:Kluwer Academic Publishers Dordrecht.

Keil, F.J., 2007. Modelling of Process Intensification. Wiley-VCH, Weinheim

Launder, B. & Spalding, D., 1974. The numerical computation of turbulent flows. Computer Methods in Applied Mechanics and Engineering, 3(2), pp. 269-289.

Mahamuni, N. N. & Adewuyi, Y. G., 2010. Application of Ultrasonic and Hydrodynamic Cavitation for Biodiesel Synthesis: A Critical. Energy & Fuels.

Musmarra, D. et al., 2016. Degradation of ibuprofen by hydrodynamic cavitation: Reaction pathways and effect of operational parameters. Ultrasonics Sonochemistry, Volume 29.

Ozonek, 2012. Application of Hydrodynamic Cavitation in Environmental Engineering. CRC Press, London.

Pandit, A. B. et al., 2015. Modeling the shear rate and pressure drop in a hydrodynamic cavitation reactor with experimental validation based on KI decomposition studies.. Ultrasonics Sonochemistry, June, Volume 22, pp. 272-277.

Pandit, A. & GaikWad, S., 2007. Application of Ultrasound in Heterogeneous Systems. Ph.D. (Tech) Thesis. s.l.:University of Mumbai.

Pandit, A., Gogate, P. & Kelkar, M., 2008. Intensification of esterification of acids for synthesis of biodiesel using acoustic and hydrodynamic cavitation. Ultrasonics, pp. 188-194.

Pandit, A., Bashir, A. & Soni, A., 2011a. The Cfd Driven Optimisation Of A Modified Venturi For Cavitational Activity. The Canadian Journal Of Chemical Engineering, 89(6), pp. 1366-1375.

Pandit, Mukherje, Kasat & Mahulkar, 2011b. Method of Designing Hydrodynamic Cavitation Reactors for Process Intensification. United States, Patent No. US 20110070639A1.

Piemonte V., Paola L.D., Gentile A., Masciocchi B., Russo V., Iaquaniello G. Biodiesel production from microalgae: Ionic liquid process simulation (2014) Chemical Engineering Transactions, 39 (Special Issue), pp. 379-384.

Piemonte V., Di Paola L., Iaquaniello G., Prisciandaro M. Biodiesel production from microalgae: Ionic liquid process simulation (2015) Journal of Cleaner Production, . Article in Press.

Rodriguez, S. et al., 2015. Effect of tribometer configuration on the analysis of hydromachinery wear failure. Wear, Volume 332-333, pp. 1164-1175.

Tarash, J., Carperter, J. & Kumar, V., 2014. CFD Analysis and Optimization of Circular and Slit Venturi for Cavitational Activity. Journal of Material Science and Mechanical Engineering (JMSME), 1(1), pp. 28-33.

Vallier, A., 2013. Simulations of cavitation – from the large vapour structures to the small bubble dynamics. Phd Thesis. Lund, Sweden: Lund University.

Versteeg, H. & Malalasekera, W., 2007. An Introduction to Computational Fluid Dynamics. 2nd ed. Harlow, England: Pearson Prentice Hall.

Wang, J. et al., 2006. Preparation of biodiesel with the help of ultrasonic and hydrodynamic cavitation. Ultrasonics, pp. 411-414.